Stearoyl-CoA desaturase-2 gene expression is required for lipid synthesis during early skin and liver development

Makoto Miyazaki*†, Agnieszka Dobrzyn*, Peter M. Elias‡§, and James M. Ntambi*†¶

Departments of *Biochemistry and ¶Nutritional Sciences, University of Wisconsin, Madison, WI 53706; ‡Department of Dermatology, University of California, San Francisco, CA 94143; and §Department of Dermatology, Veterans Affairs Medical Center, San Francisco, CA 94121

Edited by Bruce M. Spiegelman, Harvard Medical School, Boston, MA, and approved July 14, 2005 (received for review April 15, 2005)

There are four known stearoyl-CoA desaturase (SCD) enzyme isoforms in mouse and two in humans that are required for the biosynthesis of monounsaturated fatty acids, mainly oleate. SCD1 isoform plays a role in the regulation of energy metabolism and lipid synthesis, but the roles of the other SCD isoforms have not been investigated. Here we show that the SCD2 isoform is important in lipid synthesis in early development and is required for survival. SCD2-deficient (*Scd2*$^{-/-}$) neonatal mice have a skin permeability barrier defect and a specific repartitioning of linoleic acid from epidermal acylceramide species into phospholipids. *SCD2* expression is high in liver of wild-type mouse embryos and neonates between embryonic day 18.5 and 21 days of age and is decreased in adult mice. *SCD1* expression, on the other hand, is induced after weaning. The liver, skin, and plasma triglyceride contents are decreased in the neonates but are not altered in the adult *Scd2*$^{-/-}$ mice. These results indicate that, although SCD1 expression is important in adult mice, SCD2 is crucial in the synthesis of monounsaturated fatty acids that are required for maintaining normal epidermal permeability barrier function and biosynthesis of lipids during early skin and liver development.

epidermal permeability barrier | lipid metabolism

Stearoyl-CoA desaturase (SCD) is a crucial lipogenic enzyme necessary for the biosynthesis of monounsaturated fatty acids (MUFA). The major desaturation substrates are long-chain saturated acyl-CoAs such as palmitoyl (16:0)-CoA and stearoyl (18:0)-CoA, which are converted to palmitoleoyl (16:1)-CoA and oleoyl (18:1)-CoA, respectively (1). MUFA are essential components of triglycerides (TG), phospholipids, cholesteryl esters (CEs), and wax esters (2). Four isoforms of SCD have been isolated from mouse (3–6) with two human homologues (7, 8). The four mouse *SCD* genes encode proteins of 350–360 aa with >80% amino acid sequence identity, and all are located within a 200-kb region on chromosome 19 (4). In adult mice, SCD1 isoform is expressed in lipogenic tissues, including liver, adipose tissue, and sebaceous glands. SCD2 isoform is ubiquitously expressed in most tissues except liver. SCD3 expression is restricted to the sebocytes in skin, Harderian gland, and preputial gland. SCD4 is mainly expressed in the heart (3, 4, 6, 9–11).

The presence of multiple SCD isoforms that share considerable sequence homology and catalyze the same biochemical reaction makes it difficult to rationalize the role of each SCD isoform in metabolism. We are using gene knockouts in mice to determine the physiological functions of the SCD isoforms in lipid metabolism. Mice lacking the *SCD1* isoform are viable, with profound reductions in the levels of MUFA, particularly oleate, in most tissues that synthesize TG, CEs, wax esters, and alkyldiacyl glycerol (10, 12, 13). *Scd1*-deficient mice are also resistant to diet- and leptin-deficiency-induced obesity, with increased energy expenditure and insulin sensitivity (14–16). At 6 weeks old, they also develop alopecia, skin barrier abnormality, and close eye fissure with hypoplastic sebaceous and meibomian glands through a mechanism involving decreased production of wax esters, CE, and TG (13, 17, 18). These findings suggest that SCD1 plays a crucial role in lipid synthesis and regulation of energy metabolism.

To determine the biological function of SCD2 isoform, we inactivated the *SCD2* gene by homologous recombination. We report that SCD2 is important in lipid synthesis during early development and crucial for the formation of a functional skin permeability barrier. In contrast, SCD1 plays a role in lipid synthesis and energy metabolism in the later stages of life.

Materials and Methods

Generation of SCD2-Deficient Mice. Mouse genomic DNA for the targeting vector was cloned from the 129/SV genomic library (13). The targeting vector construct was generated by insertion of a fragment with 3′ homology as a short arm and a fragment with 5′ homology cloned adjacent to the neo expression cassette. The construct also contains a herpes simplex virus thymidine kinase cassette 3′ to the homology arm, allowing positive/negative selection. The targeting vector was linearized and electroporated into embryonic stem cells. Selection with geneticin and gancyclovir was performed. The targeted cells were microinjected into C57BL/6 blastocysts to generate the chimeric mice. The chimeric mice were then crossed five times with 129/SvEv (Taconic Farms) females to generate *Scd2*$^{-/-}$ mice having a genetic background of SV129. The *Scd2*$^{+/-}$ mice were also backcrossed with C57B6 mice for 10 generations to generate *SCD2*$^{-/-}$ mice on a B6 background. For PCR genotyping, genomic DNA was amplified with primer A (5′-GGGCCTG-GCTTACGACCGGAAGAGAG-3′), which is located in exon 6; primer B (5′-ATAGCAGGCATGCTGGGGAT-3′), which is located in the neo gene (570-bp product, targeted allele); and primer C (5′-GTCACGAAGTTCCTCAGTTGCCAC-3′), which is located downstream of the targeting gene (750-bp product, wild-type allele). Mice were housed in a pathogen-free barrier facility (12 h light/12 h dark cycle) and fed a standard chow diet (5008 test diet, PMI Nutrition, Richmond, IN). Newborn and 12-week-old (adult) mice were used. The committee on Animal Research of the University of Wisconsin, Madison, approved all procedures. All data shown in Figs. 1–5 were obtained by using mice in the 129Sv background.

Preparation of Epidermis. Whole skin of 1-day neonates was removed, the s.c. fat was scraped away under a dissecting microscope, and the sample was immersed in 10 mM EDTA in PBS for 1 h at 37°C. The epidermis was quickly peeled away from the dermis as described (19–21).

This paper was submitted directly (Track II) to the PNAS office.

Abbreviations: MUFA, monounsaturated fatty acid; SCD, stearoyl-CoA desaturase; Gba, β-cerebrosidase; TG, triglyceride; FFA, free fatty acid; CE, cholesteryl ester.

†To whom correspondence may be addressed. E-mail: miyazakim@biochem.wisc.edu or ntambi@biochem.wisc.edu.

RNA Analysis. Total RNA was isolated by using TRIzol reagent (Invitrogen). Fifteen micrograms of total RNA was separated by 1.0% agarose/2.2 M formaldehyde gel electrophoresis and transferred onto a nylon membrane (Millipore). The membrane was hybridized with ^{32}P-labeled *SCD* cDNAs (SCD1, -2, -3, and -4) (3–6), *β-cerebrosidase* (Gba), *transglutaminase-1*, *Involucrin*, and *Acyl-CoA:diacyl glycerol acyl transferase-2* (22) (kindly provided by R. V. Farese, Jr., Gladstone Institute, San Francisco). *SCD3* expression was measured by real-time PCR, as described (11). *pAL15* expression was used as a control.

SCD Activity. Conversion of [1-^{14}C] stearoyl-CoA to [1-^{14}C]oleate was used to measure SCD enzyme activity from individual liver and brain extracts, as described (10).

Lipid Analysis. Epidermal lipids were extracted for 24 h at 37°C in chloroform/methanol/water 1:2:0.5 (vol/vol) and then reextracted in chloroform/methanol 1:1(vol/vol) and chloroform/methanol 2:1 (vol/vol) in the presence of 100 μg/ml butylated hydroxytoluene (19). Liver lipids were extracted as described (10). The extracted total lipids were subjected to TLC (Merck Darmstadt or Whatman). For epidermal glucosylceramides and phospholipids, the TLC was developed with chloroform/methanol/water (70:30:5, vol/vol). Ceramides were resolved twice by using chloroform/methanol/acetic acid (190:9:1, vol/vol). Neutral lipids were separated with hexane/ether/acetic acid (90:30:1, vol/vol). After development, plates were dried, soaked in 8% (wt/vol) phosphoric acid containing 10% cupric sulfate, and charred at 180°C for 15 min (19). For quantitative analysis, lipids were extracted from TLC plates, and fatty acids were transmethylated and analyzed by GLC, as described (10).

Skin-Permeability Barrier Assay. Mice pups were treated with methanol at increasing concentrations of 25%, 50%, 75%, and 100% for 1 min each to modify the skin, to permit barrier-dependent penetration by histological dyes. The mice were then rinsed in PBS, followed by incubation in 0.1% toluidine blue dye, as described (19, 20).

Histological Analysis. Skin samples were taken for autopsy immediately after birth and processed for light and electron microscopy. For light microscopy, the skin was fixed in 10% neutral formaldehyde solution and embedded in paraffin. Sections were cut at 2 μm and stained with hematoxylin/eosin. For electron microscopy, samples were minced to <0.5 mm and fixed in Hepes buffer (0.16 M, pH 7.3) containing glutaraldehyde/formalin (1.25:0.5%) and 0.1 mM $CaCl_2$. Ultrathin sections were examined in an electron microscope (Zeiss 10A) (23).

Analysis of Acylceramide Synthesis in Epidermis. Epidermal sheets (20 mg) prepared from newborn mice as described above were incubated in MEM containing 10% FCS and 5 μCi (1 Ci = 37 GBq) ^{14}C-linoleic acid in 5% CO_2/95% air for 16 h. After incubation, lipids were extracted by Bligh and Dyer's method (34), and acylceramides were separated by TLC, as described above. The acylceramide fraction was scraped off the plate, and radioactivity was measured by using a liquid scintillation counter (24).

Blood Chemistries. Plasma TG and free fatty acid (FFA) concentrations were measured by gas-liquid chromatography Plasma glucose levels were determined with a glucometer (Roche Diagnostics).

Hepatic TG Synthesis. Ten microcuries of [1,2,3^{-3}H]glycerol dissolved in 0.9% NaCl was injected i.p. into newborn mice 15 min before they were killed. Hepatic lipids were extracted by using Bligh and Dyer's method and separated by TLC using hexane, ether, and acetic acid (90:30:1, vol/vol) as developing solvent. Each lipid extract was scraped off the plate, and radioactivity was measured by using a liquid scintillation counter (25).

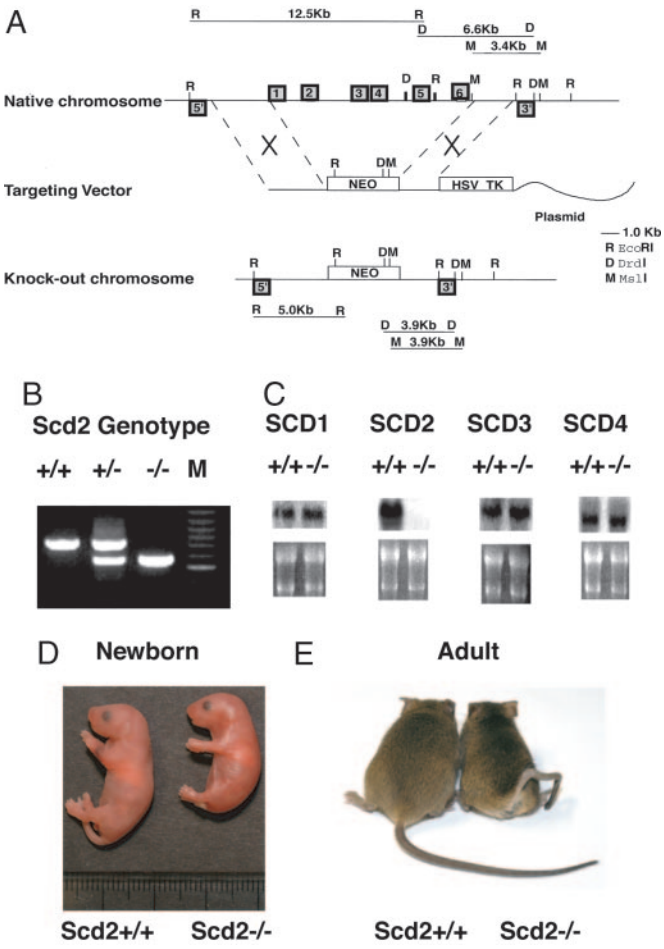

Fig. 1. Generation of *Scd2*$^{-/-}$ mice. (*A*) Targeting strategy for disruption of the *Scd2* gene. A neomycin-resistant cassette replaced the six exons of the gene by homologous recombination, resulting in the replacement of the complete coding region of the *Scd2* gene. (*B*) PCR analysis of DNA isolated from different genotypes of offspring using appropriate primers. In breeding heterozygotes, wild-type, heterozygotes and homozygotes mice were born in Mendelian fashion. (*C*) *SCD* isoform expression in adult *Scd2*$^{-/-}$ mice. *SCD1* expression was assessed in liver and brain, *SCD3* was assessed in Harderian gland, and *SCD4* expression was assessed in heart. (*D*) Gross appearance of newborn *Scd2*$^{-/-}$ mice. *Scd2*$^{-/-}$ neonatal mice were smaller in size with a shiny skin. (*E*) Adult *Scd2*$^{-/-}$ mice have a twisted tail.

Statistical Analysis. All data are expressed as means ± SD. An unpaired Student *t* test was used to determine significance.

Results

To study the role of SCD2 isoform in lipid synthesis and development, we generated *Scd2*$^{-/-}$ mice. Six exons of the gene were replaced with a neoresistant cassette by homologous recombination, resulting in the replacement of the complete coding region of the *SCD2* gene (Fig. 1*A*). This vector was used to generate embryonic stem cells and subsequently mice carrying the targeted *SCD2* allele. PCR analysis of tail genomic DNA using appropriate primers indicates that the SCD2 gene was deleted in mice (Fig. 1*B*). Because SCD isoforms are highly homologous and are located within a 200-kb region on chromosome 19, we determined whether the other *SCD* isoforms remained intact. As shown (Fig. 1*C*), very high *SCD2* expression

Table 1. Summary of the genotypes of progeny in the crossing *Scd2*$^{+/-}$ mice

Age, days	Genotype of Scd2			Number of litter	Survival rate of Scd2$^{-/-}$ mice, %
	+/+	+/−	−/−		
1	17	39	19	75	101.79
2	26	53	8	87	30.38
21	34	60	10	104	31.91

Male and female *Scd2*$^{+/-}$ mice at 8–15 weeks old were bred. Genotypes were carried out by PCR by using appropriate primers. Age shown is when mice were genotyped.

was observed in brain of wild-type but not of *Scd2*$^{-/-}$ mice. The brain of newborn and adult *Scd2*$^{-/-}$ mice showed >80% reduction in SCD activity [2.4 ± 0.5 vs. 15.7 ± 0.6 pmol/min/mg in newborn mice ($n = 4$, $P < 0.001$), 4.1 ± 0.6 vs. 44.9 ± 1.3 pmol/min/mg in adult ($n = 6$, $P < 0.01$)]. *SCD1* expression in the liver, *SCD3* expression in the Harderian gland, and *SCD4* expression in the heart were not altered in *Scd2*$^{-/-}$ mice. Genotyping of newborn from heterozygote intercrosses showed Mendelian distribution (+/+: +/−:−/− = 17:39:19), demonstrating that *SCD2* deficiency does not cause embryonic lethality. At birth, *Scd2*$^{+/-}$ mice were indistinguishable from Scd2$^{+/+}$ mice, whereas ≈70% of *Scd2*$^{-/-}$ mice on 129SvEv died within 24 h after birth (Table 1). Interestingly, 100% lethality was found in *Scd2*$^{-/-}$ mice on a pure C57Bl6 background. Newborn *Scd2*$^{-/-}$ mice were significantly smaller relative to the wild type (Fig. 1*D*, 1.16 ± 0.12 g vs. 1.38 ± 0.14 g; $n = 6$ $P < 0.001$). Adult *Scd2*$^{-/-}$ mice that survived were fertile. Adult *Scd2*$^{-/-}$ mice had a twisted tail (Fig. 1*E*), suggesting that SCD2 expression plays a role in normal mouse-tail development.

A few hours after birth, the skin of the *Scd2*$^{-/-}$ mice appeared dry and cracked. This observation suggested that *Scd2*$^{-/-}$ deficiency causes dehydration in mice and indeed, a skin-permeability assay using *o*-toluidine blue dye revealed an impairment of skin permeability barrier function in *Scd2*$^{-/-}$ mice (Fig. 2*A*). Body weights of newborn *Scd2*$^{-/-}$ mice were rapidly reduced (Fig. 2*B*), and histological examination of their skin showed an epidermal stratum corneum that was tightly packed and thickened (Fig. 2*C*). The structure of the hair follicles was normal and, unlike the *Scd1*$^{-/-}$ mice that exhibit alopecia and hypotrophic sebaceous glands, the *Scd2*$^{-/-}$ that survived to adulthood had normal sebaceous glands and hair growth. To further assess the structural basis for epidermal permeability barrier abnormality in *Scd2*$^{-/-}$ mice, we next examined the lamellar membrane system by electron microscopy (Fig. 2*D*). There are normal numbers of lamellar bodies in the *Scd2*$^{-/-}$, but a decrease in their internal contents was observed. *Scd2*$^{-/-}$ skin displayed delayed lamellar membrane maturation and phase separation forming a two-phase extracellular system. The wild-type control showed normal mature lamellar membranes in stratum corneum. The heterozygous mice did not show the skin barrier abnormalities, even though they expressed ≈50% of the *SCD2* gene (data not shown).

Because we found a decrease in the internal contents of epidermal lamellar bodies, which normally contain glucosylceramides, phospholipids, and cholesterol, we next compared the epidermal lipid composition in *Scd2*$^{-/-}$ mice vs. wild type by GLC. These analyses showed that epidermis from *Scd2*$^{-/-}$ had 37%, 76%, 44%, and 21%, respectively, decrease in the contents of CE, TG, acylceramide, and glucosylacylceramide. In contrast, the FFA content was increased 1.4-fold (Fig. 3*A*). The contents of the major phospholipids (phosphatidylcholine, phosphatidylethanolamine, and phophatidylinositol/phosphatidylserine) and free cholesterol were not different between *Scd2*$^{-/-}$ and wild-type mice. The content of oleate and palmitoleate was reduced in the total lipids (TG, cholesterol esters, acylceramides, and phospholipids) and in the FFA pool of the epidermis of *Scd2*$^{-/-}$ mice relative to the wild-type controls (Fig. 3*A* and Table 2). The content of the corresponding saturated fatty acids mainly in the FFA pool was increased. The total content of linoleic acid [18:2(*n*-6)], which is a major fatty acid of skin epidermis, was not different between the *Scd2*$^{-/-}$ mice and wild-type controls (Fig. 3*B*). However, the content of 18:2(*n*-6) was decreased by >80% in the acylceramide fraction and increased by >30% in the phospholipid fraction of the Scd2$^{-/-}$ mice relative to the controls (Table 2). These observations suggested that lack of *SCD2* causes linoleic acid deficiency in the epidermal acylceramide of the *Scd2*$^{-/-}$ mice. We then determined whether *SCD2* deficiency alters the channeling and incorporation of linoleic acid into lipid fractions. As shown in Fig. 3*C*, the acylceramide synthetic rate from trace amounts of linoleic acid was reduced by 67% in the epidermis of the *Scd2*$^{-/-}$ mice, whereas the phospholipid synthesis rate was increased by 23% (Fig. 3*D*). These data demonstrated that linoleic acid was preferentially incorporated into phospholipid rather than the acylceraimde fraction of the epidermis of *Scd2*$^{-/-}$ mice when endogenous MUFA were deficient.

To determine whether *SCD2* deficiency might affect keratinocyte differentiation and/or other genes related to skin barrier formation, we analyzed gene expression for *transglutaminase-1*, *involucrin*, *Gba*, *acyl-CoA:diacylglycerol acyltransferase-2*, *SCD1*,

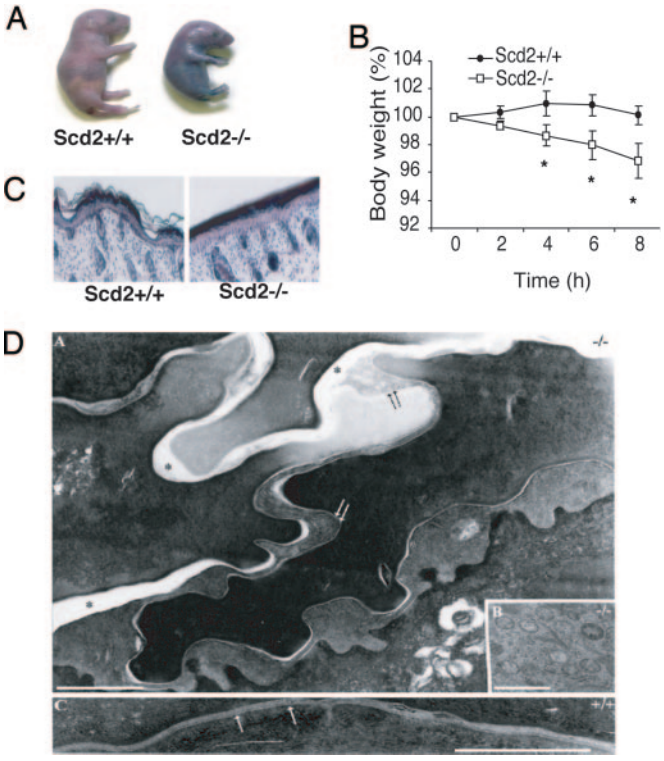

Fig. 2. Fetal impairment of the epidermal barrier in *Scd2*$^{-/-}$ mice. (*A*) Skin-permeability barrier assays using 0.1% toluidine blue. Mice were immersed in toluidine blue dye for 10 min, rinsed with PBS, and photographed. (*B*) Rapid weight loss in *Scd2*$^{-/-}$ mice is presumably due to water loss (*, $P < 0.01$, $n = 6–8$). (*C*) Light micrographs of skin of 1-day *Scd2*$^{-/-}$ mice (*Left*) in comparison with *Scd2*$^{+/+}$ mice (*Right*). (*D*) Ultrastructure of *Scd2*$^{-/-}$ epidermis. (*A*) *Scd2*$^{-/-}$ mice exhibited delayed lamellar membrane maturation (double arrow) and phase separation (asterisks), forming a two-phase extracellular system. (*B*) Lamellar bodies in the *SCD2*$^{-/-}$ mice. (*C*) The wild-type control shows normal mature lamellar membranes in stratum corneum (single arrows). (Bar, 0.5 μm.) (*A* and *C*) Ruthenium tetroxide postfixation.

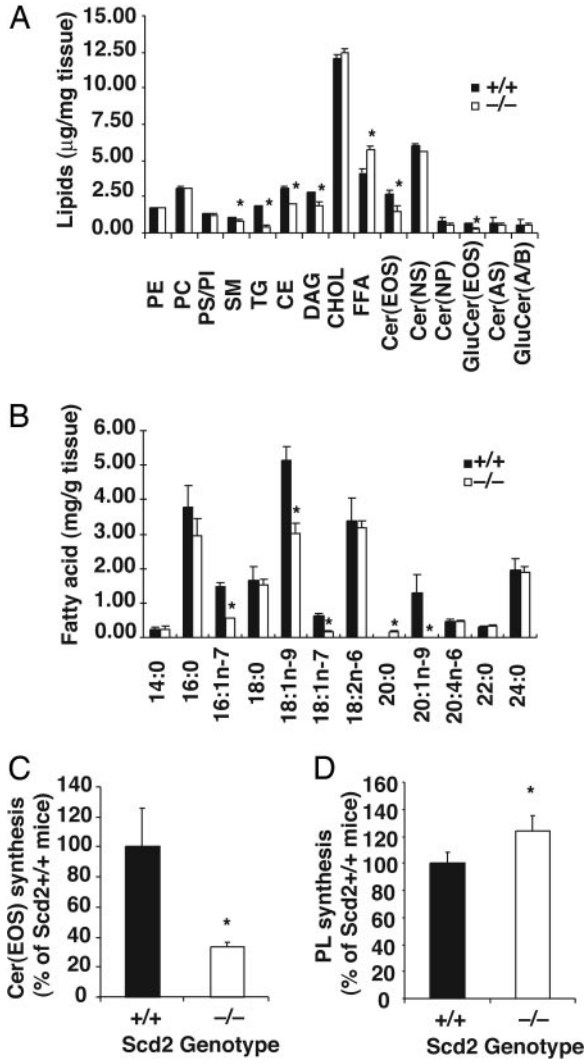

Fig. 3. Epidermal lipid contents in $Scd2^{-/-}$ mice. Lipids were extracted from epidermis (2.5 mg), separated by TLC, and quantitated by GLC. (Chol, free cholesterol; DAG, diacylglycerols; Cer, ceramides; GluCer, glucosylceramides; PE, phosphatidylethanolamine; PC, phosphatidylcholine; PS, phosphatidylserine; PI, phophatidylinositol; and SM, sphingomyelin). (*A*) Quantitations of lipids. The data are presented as the mean ± SD (n = 4–5). ∗; $P < 0.01$ vs. $Scd2^{+/+}$ mice. (*B*) Fatty acid contents in total epidermal lipids. Fatty acids were transmethylated and analyzed by GLC. n = 4~6; ∗, $P < 0.01$. (*C*) Acylceramide and (*D*) phospholipid synthesis. The incorporation of ^{14}C-linoleic acid into acylceramide and phospholipids was assessed in cultured epidermis. Epidermal sheets were organ-cultured for 12 h in MEM containing trace linoleic acid (5 μCi), and lipids were extracted as detailed in *Materials and Methods*. Data are expressed as a percentage of the values of $Scd2^{+/+}$ mice. Data are presented as the mean ± SD (n = 6); ∗, $P < 0.01$. Cer(AS), acylceramides; PL, phospholipids.

and *SCD3* in the skin of 1-day-old wild-type and $Scd2^{-/-}$ mice. Northern blot analysis showed that *SCD2* expression in epidermis and dermis of newborn *Scd2*+/+ mice was comparable (Fig. 4*A*). *SCD1* was predominantly expressed in dermis, but its expression was induced by 2.8- and 3.3-fold, respectively, in epidermis and dermis of newborn $Scd2^{-/-}$ mice, most likely to compensate for the loss of *SCD2*. *SCD3* mRNA expression was induced in epidermis but not dermis of $Scd2^{-/-}$ mice (Fig. 4*B*). The expression of keratinocyte differentiation makers, transglutaminase-1, and involucrin were reduced by 73% and 41%, respectively, in the epidermis of the $Scd2^{-/-}$ mice, whereas *Gba* and *diacylglycerol acyltransferase-2* mRNA levels that have been

Table 2. Fatty acid content of epidermis of $Scd2^{+/+}$ and $Scd2^{-/-}$ mice

Lipids	Scd2	16:0	16:1	18:0	18:1(*n*-9)	18:1(*n*-7)	18:2
PL	+/+	1,808	945	815	2,042	230	977
PL	−/−	1,885	389	811	1,122	95	1,285
FFA	+/+	769	30	212	690	38	2,324
FFA	−/−	1,213	32	252	547	36	2,697
TG	+/+	302	11	73	21	17	0
TG	−/−	204	2	77	9	3	0
CE	+/+	604	68	263	75	13	0
CE	−/−	356	38	139	43	11	0
Cer(EOS)	+/+	65	37	67	19	7	267
Cer(EOS)	−/−	88	40	67	6	0	47

Data represent the content of major fatty acid in epidermis as μg/g epidermis. Standard errors (>25% of the mean) and minor fatty acids were omitted for clarity. Underlined values are significantly different from WT mice (n = 5–6, $P < 0.05$). Cer(EOS), acylceramides; PL, phospholipids.

shown to affect skin permeability barrier development (19, 20) were similar between wild-type and $Scd2^{-/-}$ mice.

We previously demonstrated that SCD1 is a crucial enzyme for hepatic TG synthesis and energy metabolism in adult mice. To determine whether SCD2 deficiency affects hepatic lipid metabolism, we analyzed lipid levels and substrates for energy metabolism in newborn $Scd2^{-/-}$ mice. Hepatic TG contents and plasma levels were 48% (Fig. 5*A*) and 44% (Fig. 5*B*) lower in $Scd2^{-/-}$ than wild-type mice. Plasma glucose and hepatic glycogen levels were not different in $Scd2^{-/-}$ and wild-type mice (data not shown). Hepatic FFA were 27% lower in $Scd2^{-/-}$ than wild-type mice (0.77 ± 0.16 vs.1.10 ± 0.20 μmol/g $P < 0.05$). Phospholipid and CE levels were not different between $Scd2^{-/-}$ and wild-type mice. No significant differences in the contents of TG, CE, FFA, and phospholipids were observed in livers of the adult $Scd2^{-/-}$ and wild-type mice (data not shown). SCD activity was reduced by 70% in liver of newborn $Scd2^{-/-}$ mice (Fig. 5*C*), whereas the activity of adult $Scd2^{-/-}$ mice was similar to that of adult $Scd2^{+/+}$ mice (data not shown). As expected from the change in SCD activity, the contents of MUFA (palmitoleate, oleate, and vaccenate) in TG fractions of the livers of newborn $Scd2^{-/-}$ mice were decreased by 55%, 73%, and 47%, respectively (Fig. 5*D*), but in adult $Scd2^{-/-}$ mice, the contents were similar to those of wild-type mice (data not shown). The content of palmitate in TG fraction was 40% lower in the liver of newborn $Scd2^{-/-}$ mice (0.42 ± 0.05 vs. 0.25 ± 0.03 mg/g liver,

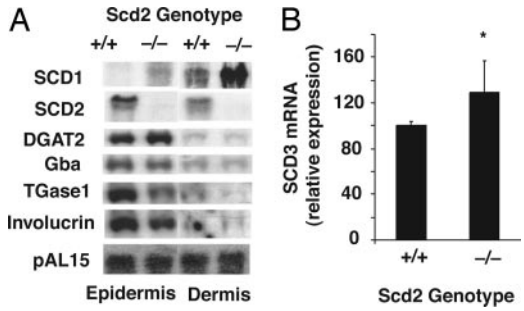

Fig. 4. Gene expression in epidermis and dermis of $Scd2^{+/+}$ and $Scd2^{-/-}$ mice. (*A*) Full thickness skin of the newborn $Scd2^{-/-}$ and $Scd2^{+/+}$ mice was removed, the s.c. fat was scraped away under a dissecting microscope, and the sample was immersed in 10 mM EDTA in PBS for 1 h at 37°C. The skin was then chilled on ice, and the epidermis was quickly peeled away from the dermis. RNA was isolated from the epidermis and dermis and analyzed by Northern blot for expression of *SCD1*, *SCD2*, *acyl-CoA:diacylglycerol acyl transferase-2*, *Gba*, and *involucrin*. *pAL15* expression was used as loading control. (*B*) *SCD3* mRNA levels were measured by real-time PCR. ∗, $P < 0.05$ vs. $Scd2^{+/+}$ mice (n = 4~6).

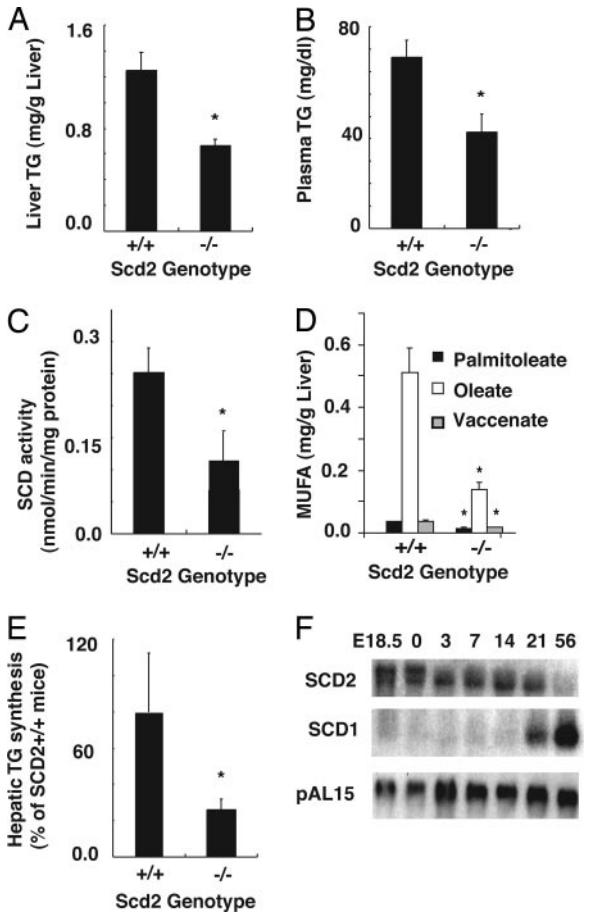

Fig. 5. Hepatic and plasma TG levels and hepatic SCD activity in newborn mice. (*A*) Hepatic and (*B*) plasma TG contents were analyzed by GLC. (*C*) SCD activity was measured as conversion rate of [^{14}C]18:0-CoA to [^{14}C]-18:1-CoA. (*D*) MUFA levels in TG in liver of newborn and adult mice. Palmitoleate [16:1(*n*-7)], oleate [18:1(*n*-9)], and vaccenate [18:1(*n*-7)] contents in TG were measured by GLC. (*E*) Rate of TG synthesis in liver of newborn mice. Mice were i.p. injected with 10 μCi of ^{3}H-glycerol 1 h before being killed. After extraction of hepatic lipids, TG and phospholipids were separated by TLC, and radioactivity was determined. Data are expressed as a percentage of the values of *Scd2*$^{+/+}$ mice). *, $P < 0.01$ vs. *Scd2*$^{+/+}$ mice ($n = 6$). (*F*) Developmental expression of *SCD1* and *-2* in mouse liver. The expression level of *SCD1* and *-2* in liver of mice at embryonic day 18.5, newborn, and 3, 7, 14, 21, and 56 days of age was measured by Northern blot analysis. Expression levels were obtained from pooled total RNA from four to five mice. *pAL15* mRNA was used as a loading control.

$n = 5, P < 0.05$), but there were no significant differences in the contents of other fatty acids (data not shown).

To determine whether *SCD2* deficiency affects lipid synthesis in liver, we examined the *in vivo* synthesis rate of lipids by measuring the incorporation of i.p.-injected ^{3}H-glycerol into TG and phospholipids. The liver of newborn *Scd2*$^{-/-}$ mice showed 54% reduction in TG synthesis rate relative to newborn *Scd2*$^{+/+}$ mice (Fig. 5*E*). In contrast, there was no difference in hepatic TG synthesis between adult *Scd2*$^{-/-}$ and *Scd2*$^{+/+}$ mice. The incorporation of ^{3}H-glycerol into the phospholipid fraction was not different between *Scd2*$^{-/-}$, wild-type newborn and adult mice (data not shown). This result suggests that *SCD2* expression is important in TG synthesis in liver of neonates. To determine the developmental expression of the *SCD* genes, we analyzed the changes in hepatic expression of *SCD1* and *SCD2* in embryos, neonates, and adult wild-type mice. Fig. 5*F* shows that *SCD2* mRNA expression is high in livers of mouse embryos and neonates between embryonic day 18.5 and 21 days of age and decreases in adult mice. On the other hand, *SCD1* expression is very low in neonates and is induced after weaning (day 21). *SCD3* and *-4* expression was not detectable in liver.

Discussion

The mouse genome contains four well characterized Δ-9 desaturase genes (SCD1–4) that are highly homologous at the nucleotide and amino acid levels and encode the same functional protein. The difference in biological function and the reasons for the existence of the multi-SCD isoforms in the mouse genome have not been addressed. Previous studies of mice with a disruption in the *SCD1* gene isoform demonstrated that SCD1 and oleate, its major product, could act as a metabolic switch that increases fat synthesis and storage when SCD1 expression is high and conversely enhances fat oxidation when SCD1 expression is low. One of the consequences of this metabolic switch would be to protect mice against liver steatosis and diet- and leptin-induced obesity. In this study, we show that the SCD2 isoform plays a major role in lipid synthesis and metabolism in early skin and liver development and is important for survival, whereas SCD1 expression appears to be more important later in development.

Although *Scd2*$^{-/-}$ mice were born in the expected Mendelian manner, most of the mice died within 24 h after birth, most likely as a result of severe dehydration due to skin permeability barrier dysfunction. The mechanism by which *SCD2* deficiency leads to defective permeability barrier function is most probably due to alterations in epidermal lipid metabolism. Electron microscopic analysis of the epidermal stratum corneum of the *Scd2*$^{-/-}$ mice revealed immature lamellar membranes and reductions in the internal contents of epidermal lamellar bodies, suggesting impaired delivery of lipid to lamellar granules, leading to insufficient deposition of lipids in the stratum corneum interstices. It has been known that the precursors of the striatum corneum lipids in lamellar granules are mainly cholesterol, phospholipids, and glucosylceramides (26, 27). In agreement with EM analysis, lipid analysis showed that the content of glucosylceramide was significantly reduced in *Scd2*$^{-/-}$ mice despite no alterations in the content of either phospholipids or cholesterol. Further conversion of epidermal glycosylceramides and acylglycosylceramides to ceramides and acylceramides, respectively, by Gba is required for skin permeability barrier homeostasis (19). The amount of acylceramide, a unique and essential epidermal lipid (26, 27), was reduced by 30% in the epidermis of *Scd2*$^{-/-}$ mice, despite no alteration in Gba expression. Recently, Stone *et al.* (20, 22) reported that mice lacking diacylglycerol acyltransferase-2, a rate-limiting enzyme of TG synthesis, exhibited defective skin permeability barrier with lethality similar to *Scd2*$^{-/-}$ mice. We also found a drastic reduction of TG and CE in the epidermis of *Scd2*$^{-/-}$ neonatal mice, although the expression of epidermal *diacylglycerol acyl transferase-2* was not altered. Thus, our results suggest that the reduction in lipid contents, including acylceramide, TG, and CE, in the epidermis of *Scd2*$^{-/-}$ mice is due to lack of sufficient levels of endogenous MUFA.

Some aspects of the skin phenotype of *Scd2*$^{-/-}$ mice resemble essential fatty acid deficiency that has been known to exist in mouse skin for decades. In this model, it has been postulated that linoleic acid [18:2(*n*-6)] is replaced by the accumulation of 20:3(*n*-9), which is an elongation and desaturation product of 18:1(*n*-9). Essential fatty acids are required for normal growth and skin function, and a deficiency in these fatty acids is characterized by growth retardation, skin abnormalities, and increased transepidermal water loss. In addition, linoleic acid is the major component of acylceramide, the major lipid involved in epidermal permeability barrier function (28–30). Analysis of fatty acid composition of epidermal lipids showed that, although the total amounts of linoleic acid in the lipid fractions and FFA

pool were not different between $Scd2^{+/+}$ and $Scd2^{-/-}$ mice, the content of linoleic acid in acylceramide was reduced by >80%, whereas that in the phospholipid fraction was increased by >30%. In addition, very little linoleic acid was detected in TG and CE fractions of epidermis of either $Scd2^{-/-}$ or wild-type mice. The mechanism consistent with our observations is that for $Scd2^{-/-}$ mice to compensate for the reduction in the levels of MUFA required for the synthesis of phospholipids to maintain membrane fluidity and cell structure, linoleic acid coming into the embryo from maternal plasma is partitioned away from acylceramide synthesis into phospholipid synthesis. The reduced levels of acylceramide and deficiency of linoleic acid in the acylceramide fraction would be consistent with a skin permeability barrier defect in the $Scd2^{-/-}$ mice. The mechanism of how the decision is made to partition linoleic acid is not known but is probably at the level of enzymes that activate linoleic acid before channeling into the phospholipid fraction and other metabolic pathways.

The expression of *SCD1* was induced in the epidermis of $Scd2^{-/-}$ neonates (Fig. 4), and it is possible those mice that had the highest induction produced adequate amounts of MUFA that overcame the linoleic acid deficiency in the acylceramide fraction and had a functional skin permeability barrier. The degree of *SCD1* induction in skin of $Scd2^{-/-}$ mice was varied, and $Scd2^{-/-}/Scd1^{+/-}$ double mutant mice on 129 background showed 100% lethality (data not shown), suggesting that adequate levels of SCD1 expression in the skin were required for survival of the 30% of the $Scd2^{-/-}$ mice that made it to adulthood. The epidermis of $Scd2^{-/-}$ mice exhibited a reduction in the expression of involucrin and transglutaminase-1, makers of mature keratinocytes (31–33), suggesting that *SCD2* deficiency attenuates keratinocyte differentiation. Thus SCD2, as well as its products MUFA, may play a crucial role in keratinocyte differentiation and skin homeostasis in neonatal mice. Further experiments will be required to address this point.

We found that SCD2, but not SCD1, controls MUFA and TG synthesis in liver of neonatal mice. Because it has been well known that SCD2 expression is very low in adult liver (3, 4), except in leptin-deficient adult *ob/ob* mice (unpublished data), we therefore expected to observe no phenotype in liver of adult $Scd2^{-/-}$ mice. Indeed, in livers of adult $Scd2^{-/-}$ mice that survived, there was no change in *SCD1* expression, SCD activity, fatty acid composition, and hepatic and plasma TG contents when compared with $Scd2^{+/+}$ mice. However, newborn $Scd2^{-/-}$ showed decreases in hepatic SCD activity, MUFA, and hepatic and plasma TG contents. SCD2 is therefore a major isoform in liver of embryos and neonates and, consistent with its role in early development, its expression in liver was decreased before weaning and replaced by *SCD1* at the weaning age (Fig. 5*F*). We have also shown previously (12, 14) that in $Scd1^{-/-}$ mice, the levels of hepatic TG and MUFA decrease as the mice age. Together, the results clearly show that SCD2 plays a crucial role in hepatic TG synthesis in early stages of life, whereas SCD1 expression is required in later stages. Although the mechanism of how *SCD2* isoform is switched off and *SCD1* is switched on during development has not been determined, many dietary nutrients, including vitamins, polyunsaturated fatty acids, and carbohydrates, which are known to influence *SCD1* and *SCD2* expression, might be involved in this isoform shift at weaning.

Two isoforms of SCD (SCD1 and -5) have been identified in the human genome (7, 8). Based on its tissue distribution, it seems that human SCD5 plays a similar developmental role in lipid metabolism as mouse SCD2. In humans, a pericentric inversion of the *SCD5* localized at chromosome 4 was found in two generations in a family with cleft lip, a common birth defect in humans (7). Although no cleft-lip phenotype was observed in $Scd2^{-/-}$ mice, we found an abnormal shape of tail in $Scd2^{-/-}$ mice. Thus, MUFA due to SCD2 expression play a role in developmental processes in mouse. Based on our previous studies, SCD1 still remains a potential target in the treatment of liver steatosis, obesity, and diabetes in adult humans. The development of a selective inhibitor of SCD isoforms at the different stages of development would even be better.

We thank Dr. M. Flowers for critical review of the manuscript and W. C. Man, H. Sampath, and K. Chu for helpful discussions. This work was supported by the National Institute of Diabetes and Digestive and Kidney Diseases, National Institutes of Health Grant RO1162388 (to J.M.N.).

1. Enoch, H. G., Catala, A. & Strittmatter, P. (1976) *J. Biol. Chem.* **251,** 5095–5103.
2. Miyazaki, M. & Ntambi, J. M. (2003) *Prostaglandins Leukotrienes Essent. Fatty Acids* **68,** 113–121.
3. Kaestner, K. H., Ntambi, J. M., Kelly, T. J., Jr., & Lane, M. D. (1989) *J. Biol. Chem.* **264,** 14755–14761.
4. Miyazaki, M., Jacobson, M. J., Man, W. C., Cohen, P., Asilmaz, E., Friedman, J. M. & Ntambi, J. M. (2003) *J. Biol. Chem.* **278,** 33904–33911.
5. Ntambi, J. M., Buhrow, S. A., Kaestner, K. H., Christy, R. J., Sibley, E., Kelly, T. J., Jr., & Lane, M. D. (1988) *J. Biol. Chem.* **263,** 17291–17300.
6. Zheng, Y., Prouty, S. M., Harmon, A., Sundberg, J. P., Stenn, K. S. & Parimoo, S. (2001) *Genomics* **71,** 182–191.
7. Beiraghi, S., Zhou, M., Talmadge, C. B., Went-Sumegi, N., Davis, J. R., Huang, D., Saal, H., Seemayer, T. A. & Sumegi, J. (2003) *Gene* **309,** 11–21.
8. Zhang, L., Ge, L., Parimoo, S., Stenn, K. & Prouty, S. M. (1999) *Biochem. J.* **340,** 255–264.
9. Ntambi, J. M. (1995) *Prog. Lipid Res.* **34,** 139–150.
10. Miyazaki, M., Kim, H. J., Man, W. C. & Ntambi, J. M. (2001) *J. Biol. Chem.* **276,** 39455–39461.
11. Miyazaki, M., Gomez, F. E. & Ntambi, J. M. (2002) *J. Lipid Res.* **43,** 2146–2154.
12. Miyazaki, M., Kim, Y. C., Gray-Keller, M. P., Attie, A. D. & Ntambi, J. M. (2000) *J. Biol. Chem.* **275,** 30132–30138.
13. Miyazaki, M., Man, W. C. & Ntambi, J. M. (2001) *J. Nutr.* **131(9),** 2260–2268.
14. Cohen, P., Miyazaki, M., Socci, N. D., Hagge-Greenberg, A., Liedtke, W., Soukas, A. A., Sharma, R., Hudgins, L. C., Ntambi, J. M. & Friedman, J. M. (2002) *Science* **297,** 240–243.
15. Ntambi, J. M., Miyazaki, M., Stoehr, J. P., Lan, H., Kendziorski, C. M., Yandell, B. S., Song, Y., Cohen, P., Friedman, J. M. & Attie, A. D. (2002) *Proc. Natl. Acad. Sci. USA* **99,** 11482–11486.
16. Rahman, S. M., Dobrzyn, A., Dobrzyn, P., Lee, S., Ntambi, J. M. & Miyazaki, M. (2003) *Proc. Natl. Acad. Sci. USA* **100,** 11110–11115.
17. Sundberg, J. P., Boggess, D., Sundberg, B. A., Eilertsen, K., Parimoo, S., Filippi, M. & Stenn, K. (2000) *Am. J. Pathol.* **156,** 2067–2075.
18. Zheng, Y., Eilertsen, K. J., Ge, L., Zhang, L., Sundberg, J. P., Prouty, S. M., Stenn, K. S. & Parimoo, S. (1999) *Nat. Genet.* **23,** 268–270.
19. Doering, T., Holleran, W. M., Potratz, A., Vielhaber, G., Elias, P. M., Suzuki, K. & Sandhoff, K. (1999) *J. Biol. Chem.* **274,** 11038–11045.
20. Stone, S. J., Myers, H. M., Watkins, S. M., Brown, B. E., Feingold, K. R., Elias, P. M. & Farese, R. V., Jr. (2004) *J. Biol. Chem.* **279,** 11767–11776.
21. Takagi, S., Tojo, H., Tomita, S., Sano, S., Itami, S., Hara, M., Inoue, S., Horie, K., Kondoh, G., Hosokawa, K., *et al.* (2003) *J. Clin. Invest.* **112,** 1372–1382.
22. Cases, S., Stone, S. J., Zhou, P., Yen, E., Tow, B., Lardizabal, K. D., Voelker, T. & Farese, R. V., Jr. (2001) *J. Biol. Chem.* **276,** 38870–38876.
23. Hou, S. Y., Mitra, A. K., White, S. H., Menon, G. K., Ghadially, R. & Elias, P. M. (1991) *J. Invest. Dermatol.* **96,** 215–223.
24. Takagi, Y., Nakagawa, H., Matsuo, N., Nomura, T., Takizawa, M. & Imokawa, G. (2004) *J. Invest. Dermatol.* **122,** 722–729.
25. Miyazaki, M., Kim, Y. C. & Ntambi, J. M. (2001) *J. Lipid Res.* **42,** 1018–1024.
26. Wertz, P. W. (2000) *Acta Dermatol. Venereol. Suppl.* **208,** 7–11.
27. Madison, K. C. (2003) *J. Invest. Dermatol.* **121,** 231–241.
28. Hansen, H. S. & Jensen, B. (1985) *Biochim. Biophys. Acta* **834,** 357–363.
29. Melton, J. L., Wertz, P. W., Swartzendruber, D. C. & Downing, D. T. (1987) *Biochim. Biophys. Acta* **921,** 191–197.
30. Wertz, P. W. & Downing, D. T. (1990) *J. Lipid Res.* **31,** 1839–1844.
31. Schmuth, M., Elias, P. M., Hanley, K., Lau, P., Moser, A., Willson, T. M., Bikle, D. D. & Feingold, K. R. (2004) *J. Invest. Dermatol.* **123,** 41–48.
32. Tu, C. L., Chang, W. & Bikle, D. D. (2001) *J. Biol. Chem.* **276,** 41079–41085.
33. Mao-Qiang, M., Fowler, A. J., Schmuth, M., Lau, P., Chang, S., Brown, B. E., Moser, A. H., Michalik, L., Desvergne, B., Wahli, W., *et al.* (2004) *J. Invest. Dermatol.* **123,** 305–312.
34. Bligh, E. G. & Dyer, W. J. (1959) *Can. J. Med. Sci.* **37,** 911–917.